*Environ. Sci. Technol.* **2006**, *40,* 945−954

# Effects of Sampling Artifacts and Operating Parameters on the Performance of a Semicontinuous Particulate Elemental Carbon/ Organic Carbon Monitor

MOHAMMAD ARHAMI, THOMAS KUHN, PHILIP M. FINE, RALPH J. DELFINO, AND CONSTANTINOS SIOUTAS*

*Department of Civil and Environmental Engineering, University of Southern California, 3620 South Vermont Avenue, Los Angeles, California 90089*

The carbonaceous component of atmospheric particulate matter (PM) is considered very important with respect to the observed adverse health effects of PM. Particulate organic and elemental carbon have traditionally been measured off-line after daily, time-integrated particle collection on filters. However, the subdaily or hourly variability of elemental carbon (EC) and organic carbon (OC) can help to assess the variability of sources, ambient levels, and human exposure. In this study, the performance of the Sunset Laboratory Inc. semicontinuous EC/OC monitor was assessed in a Los Angeles location representing typical urban pollution. An intermonitor comparison showed high precision ($R^2$ of 0.98 and 0.97 for thermal OC and EC, respectively). By changing the inlet configurations of one of the monitors (adding a denuder, a Teflon filter, or both), the influences of positive and negative sampling artifacts were investigated. The positive artifact was found to be relatively large (7.59 $\mu$g/m$^3$ on average), more than 50% of measured OC, but it was practically eliminated with a denuder. The negative artifact was much smaller (less than 20% of the positive artifact) and may be neglected in most cases. A comparison of different temperature profiles, including a fast 4-min analysis using optical EC correction, showed good agreement among methods. Finally, a novel configuration using a size selective inlet impactor removing particles greater than 250 nm in diameter allowed for semicontinuous size-fractionated EC/OC measurements. Evolution of OC at different temperatures of the thermal analysis showed higher volatility OC in larger particles.

## Introduction

While the link between ambient fine particle mass ($PM_{2.5}$) and adverse health outcomes has now been repeatedly established (*1*), it is still not fully understood which properties of airborne particles are most responsible for these observations. Various studies have implicated sulfate (*2*, *3*); toxic elements such as vanadium (*4*), silicon (*5*), iron, nickel, and zinc (*6*); elemental carbon (*7*, *8*); organic compounds such as polycyclic aromatic hydrocarbons (*9*); ultrafine particles (diameters less than ∼180 nm) (*10*, *11*); wood smoke (*12*); and diesel exhaust (*13*), to name only a few. Therefore, accurate and convenient instruments, which measure detailed particle characteristics, are necessary to better assess ambient concentrations and human exposures. Continuous or semicontinuous monitors, providing data on hourly or subhourly time scales, are generally preferred over off-line analyses. Such monitors can not only capture important short-term variations in particle properties, but also can prove more economical to operate by reducing sampling site visits and eliminating the need for laboratory facilities and analysis costs.

The carbonaceous component of atmospheric aerosols, elemental carbon (EC), organic carbon (OC), and carbonate (*14*, *15*), has been considered one of the most relevant PM fractions with respect to observed adverse health outcomes. Carbonate does not comprise a significant portion of $PM_{2.5}$ and is not suspected of being toxicologically active. Elemental carbon, similar to black carbon or refractory carbon (*14*, *16*), is emitted from incomplete combustion occurring in sources such as diesel engines and biomass burning. It has been shown to produce adverse health responses when inhaled in both laboratory and ambient studies (*7*, *8*, *17*). Particulate organic carbon is a component of particles emitted from almost every known primary particle source (*18*), but it also can consist of secondary organic aerosol (SOA) formed in the atmosphere (*19*). Both primary and secondary OC consist of hundreds of organic species, many of which are known to be toxic (i.e. PAH, nitro-PAH, etc.) (*20*, *21*). The particle size distributions of both EC and OC are generally shifted to lower particle diameters relative to the total PM mass size distribution (*22*).

The OC and EC components of PM have traditionally been measured off-line after particle collection on filters (*14*, *16*). Numerous analytical methods have been developed, including thermal evolution techniques that heat the filter to high temperatures and measure the total carbon that evolves off the filter. During heating, a portion of organic carbon pyrolizes to form elemental carbon. Some of the methods use both nonoxidizing and oxidizing atmospheres and, by optically monitoring filter appearance, attempt to correct for this pyrolysis (*14*, *16*). Several studies have examined the accuracy of these methods (*23*−*27*). For the pyrolysis-corrected techniques, it was found that the temperature profile and the laser configuration, reflectance vs transmittance, affected the results. Off-line analysis techniques are applied to time-integrated filters that typically collect PM for 24 h or longer. However, these methods do not provide potentially useful information on the variability of EC and OC found in subdaily or hourly data. Such data provided on finer temporal scales can help to assess the variability of sources, ambient levels, and human exposure to EC and OC.

To address this need, several in-situ continuous or semicontinuous particle measurement instruments have been developed for the measurement of EC, OC, or both. Black carbon can be measured continuously with an Aethalometer, which measures the absorption of single-wavelength light through a filter collecting airborne particles (*28*). Thermal evolution carbon monitors have been deployed in the field as well (*29*, *30*). The Sunset Laboratories Inc. semicontinuous EC/OC monitor was evaluated in a field study in St. Louis (*30*). In that study, OC levels were shown to agree very well with off-line OC measurements of 24-h time-integrated filters using the laboratory-based Sunset Lab analyzer ($R^2 = 0.90$, slope = 0.93). EC comparisons showed less agreement, most

* Corresponding author fax: 213-744-1426; e-mail address: sioutas@usc.edu.

10.1021/es0510313 CCC: $33.50 
Published on Web 12/15/2005

likely due to the very low ambient EC concentrations encountered at that sampling site. Since these instruments require an analysis cycle during which sample is not collected, this study used two monitors to sample alternating hours to achieve full 24-h collection. However, a single instrument sampling every other hour yielded good agreement with 24-h time-integrated off-line methods.

Collecting particles on filters, either on-line or off-line, potentially leads to sampling artifacts. A positive organic carbon artifact arises from organic vapor adsorption onto quartz-fiber filter material and previously collected particles (matrix), leading to an overestimation of particle phase OC (*31*, *32*). A negative artifact can be caused by volatilization of organic particle-phase semivolatile compounds from the particles into the gas phase, leading to an underestimation of OC (*31*).

The objective of our study was to further assess the performance of the Sunset Lab semicontinuous EC/OC monitor in a field setting. Two identical and collocated instruments were run concurrently on a cycle consisting of 45 min of sampling and 15 min of analysis. The monitors were deployed near downtown Los Angeles at the Southern California Supersite Particle Instrumentation Unit (PIU) trailer. The location is about 100 m downwind of a major freeway, is surrounded by multistory buildings, is near a construction area, and represents a good urban pollution mix (*33*). The collocated identical configurations allowed for the evaluation of the intermonitor precision and the effects of monitor maintenance such as filter changes. By changing the inlet configurations of one of the monitors (adding a denuder, a Teflon filter, or both), the influences of positive and negative sampling artifacts were investigated. The temperature profiles were also varied between instruments, including a fast 4-min analysis using an optical EC calibration rather than the thermal EC measurements. Finally, a novel configuration using a size-selective inlet impactor removing particles greater than 250 nm in diameter allowed for semicontinuous size-fractionated EC/OC measurements. Observations of the evolution of OC at different temperatures of the thermal analysis also provided data on the relative volatility of OC in particles of different sizes.

## Experimental Methods

**Semicontinuous OC/EC Field Instruments.** Two identical OC/EC field instruments (Model 3F, Sunset Laboratory, Inc., Portland, OR) were deployed for monitoring the carbonaceous components of PM between December 2004 and May 2005. These instruments provide for automated sample collection and analysis of OC and EC on a semicontinuous basis (*30*). Samples are collected by drawing a sample flow of 8 L/min through two round 16-mm quartz filters, which are mounted back to back in an oven inside the instrument. After sample collection, the sample remains in the oven, where it is heated in two different steps. First, the oven is purged with helium and the temperature is increased in multiple steps based on the programmed temperature profile. The evolved organic carbon flows through a manganese dioxide ($MnO_2$) oxidizing oven and all carbon is transformed in to carbon dioxide ($CO_2$) (*30*, *34*). The $CO_2$ is then quantified by a self-contained nondisperse infrared (NDIR) detector (*35*). The oven is cooled prior to the second part of the analysis, when the oven is purged with a mixture of 10% oxygen in helium and the sample is again heated in steps (*30*, *34*). During this stage, all remaining carbon on the filter, including elemental carbon, is oxidized, flows through the $MnO_2$ oven, and is detected by NDIR as $CO_2$.

During the first part of analysis, a fraction of organic compounds may pyrolyze and form EC (*30*, *34*). This pyrolitic conversion is monitored by continuous measurement of the light absorbance of a red laser (wavelength of 660 nm) passed through the filter. The light absorbance increases as some OC is pyrolized to EC during the first analysis stage, and then the absorbance declines as EC (from both pyrolized OC and sampled particles) is oxidized and leaves the filter during the second stage. The point at which the laser absorbance equals the initial value is considered the split point between OC and EC (*14*, *30*, *36*).

The instruments also provide an optical determination of EC. The laser transmission is measured before and after the analysis cycle, and the difference is related to EC concentration via calibration. A predetermined calibration factor, based on numerous ambient measurements, is used to convert laser attenuation to EC mass on the filter (*34*). This optical EC is subtracted from the thermally measured total carbon (TC = EC + OC) to determine a parameter known as optical OC. All the EC and OC results presented in this study are thermal OC and EC unless stated otherwise.

Some refractory inorganic particle components not removed in the heating process will accumulate on the filters. This is observed in the diminished initial laser transmittance through the filter over several days of sampling. The effect of using a week-old filter versus a fresh filter on the measured OC and EC was examined in this study and shown to be negligible. However, the filters were changed once a week as recommended by the manufacturer. The instruments were initially calibrated by injecting 1 $cm^3$ of calibration gas into the analyzers two times during the analysis period. The stability of the analyzers was checked by the same method later during the study period. Good internal instrumental stability was observed, as was also shown in a previous study (*30*).

**Sampling Description.** The instruments were operated in a sampling trailer and sampled ambient air from a common inlet located on the roof. Inside the trailer, the common intake flow was split between the two instruments. Each instrument was operated downstream of its own $PM_{2.5}$ cyclone (provided by the manufacturer) at a flow rate of 8 L/min. The analyzers were run concurrently in coordinated hourly cycles, which included a 45-min sampling period and a 15-min analysis period. A previous study using the same monitors showed good agreement between measurements made every other hour and 24-h time-integrated off-line methods with $R^2 = 0.89$ and a slope of 0.94 for OC (*30*). Thus, missing half of the sampling time did not significantly bias 24-h results. By extension, the 15 min of analysis during which sampling is interrupted should not significantly bias what is subsequently referred to as hourly readings.

The sampling location was on the University of Southern California campus at the Southern California Supersite PIU trailer. This site is located near downtown Los Angeles with a major freeway located about 100 m upwind (*33*). The site is surrounded by several multistory buildings and is near a construction area. The air at this site represents a typical urban mix of mobile, industrial, and construction sources (*33*). An Aethalometer [Model AE-21 (UV + BC), Thermo Andersen, Smyrna, GA] was deployed at the same location and measured black carbon (BC) in 5-min averages.

The different sampling configurations used in this study are presented in Figure 1. Two of these five configurations (configuration A−E) were run concurrently during each of the sampling periods. The OC and EC measured via these configurations are referred to as $OC_A$, $OC_B$, ..., $OC_E$ and $EC_A$, $EC_B$, ..., $EC_E$ based on the inlet configuration employed. All configurations used the manufacturer supplied $PM_{2.5}$ cyclone.

**Precision Evaluation.** The precision of the instruments was tested via side-by-side operation, using only the cyclone on the inlet (bare configuration, Figure 1a). Each instrument collected 182 hourly samples in January 2005, and the OC and EC measured with the two analyzers were compared. Also, an evaluation of the optical EC and OC measurements

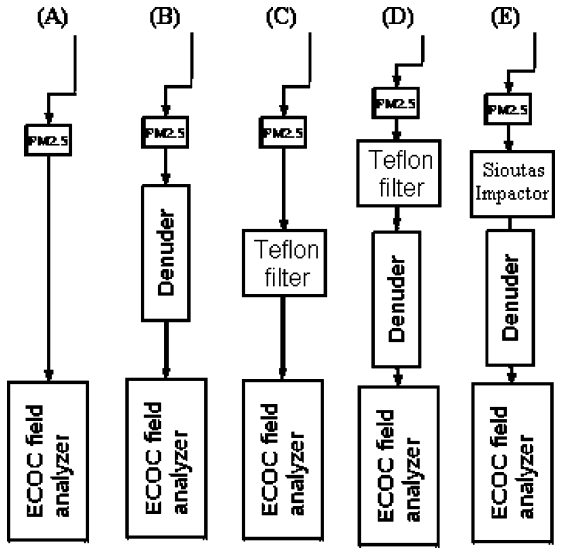


**FIGURE 1. Inlet configurations implemented for sampling: (A) bare, (B) denuded, (C) filtered, (D) denuded/filtered, and (E) quasi-ultrafine.**

were compared to their thermal counterparts using the instruments in the bare configuration. The BC measurements from the Aethalometer are often comparable to EC measurements (*28*, *29*, *36*−*38*), and the hourly averages of BC measured by Aethalometer were compared to the EC results of the Sunset Laboratory monitors.

**Denuder Breakthrough Determination.** A carbon-paper denuder (provided by the manufacturer) was used to remove gas-phase OC that is known to cause positive adsorption artifacts (*39*). The efficiency of a denuder can be less than 100%, allowing some organic gases to penetrate through the denuder (breakthrough) (*31*). The denuder breakthrough was measured by installing a 47-mm Teflon filter (PTFE, Gelman, 2-$\mu$m pore, Ann Arbor, MI) followed by the carbon-paper denuder upstream of the samplers (Figure 1d). The Teflon filter removes the particles and the denuder removes organic vapors from the air stream (*30*, *31*, *39*). EC measurements under this configuration ($EC_D$) were practically zero, demonstrating complete removal of particles by the Teflon filter. Thus, the measured value of organic carbon ($OC_D$) is due to organic gases penetrating through the denuder and adsorbing on the quartz filter. Since the measured $OC_D$ values were fairly consistent (see Results and Discussion), the average of the breakthrough level was subtracted from all subsequent OC measurements using the denuder. This denuder breakthrough value is specific to this type of denuder; different breakthrough values are expected if other types of denuders are used. The effect of the age of the carbon-paper strips in the denuder on breakthrough was assessed by side-by-side comparison of a denuder with fresh strips and one with 2-month-old strips. The results did not show a significant change after denuder strips were changed. Denuder strips were deployed a maximum of 3 months before replacement with fresh strips.

**Artifact Measurements.** Two different methods were used for examining the magnitude of positive and negative sampling artifacts: a denuder method and a filter method. For the denuder method, an instrument with the denuder setup (configuration B, Figure 1b) was run side-by-side with the other instrument in the bare configuration A (Figure 1a) in January 2005. The denuder removes the organic vapors that may cause a positive adsorption artifact (*30*, *31*). However, it may increase the magnitude of negative volatilization artifacts, since lowered organic vapor pressures favor volatilization of organic carbon from particles already collected on the filter (*40*, *41*). The measured organic carbon with the denuder configuration ($OC_B$), after correction for breakthrough, would be equal to actual particulate OC ($OC_{actual}$) minus the negative artifact. The measured organic carbon via the bare measurement ($OC_A$) is $OC_{actual}$ plus the positive artifact, since no significant negative artifact is expected for the bare configuration during such short sampling periods (*31*). Thus, the difference between $OC_A$ and $OC_B$ is an estimate of the positive artifact plus the negative artifact and is referred to as the total artifact determined via the denuder method ($OC_{artifact,denuder} = OC_A - OC_B$).

**TABLE 1. Temperature Profiles Used for EC/OC Analysis**

| | | temperature (°C) | |
|---|---|---|---|
| gas | hold time (s) | modified-NIOSH | modified-IMPROVE |
| He | 10 | no heating | no heating |
| He | 60 | 310 | 120 |
| He | 60 | 480 | 250 |
| He | 60 | 615 | 450 |
| He | 90 | 840 | 550 |
| He | 35 | no heating | no heating |
| He+Ox | 35 | 550 | 550 |
| He+Ox | 105 | 850 | 850 |

| gas | hold time (s) | FAST-ramp temp (°C) |
|---|---|---|
| He+Ox | 10 | no heating |
| He+Ox | 210 | 850 |

In the filter method, a 47-mm Teflon filter was installed downstream of the cyclone of one of the EC/OC analyzers (configuration C, Figure 1c) and run side-by-side with the other instrument in the bare configuration in December 2004. The Teflon filter prevents particles from entering the instrument so that the measured carbon content is entirely due to adsorbed gas-phase organics (*30*, *31*, *39*). It is therefore a direct measure of the positive artifact as determined with the filter method ($OC_{artifact,filter} = OC_C$) (*30*, *31*). Near-zero $EC_C$ levels confirmed the effectiveness of the filter. The measured $OC_C$ was subtracted from the concurrent $OC_A$, and the results are taken as actual particulate OC ($OC_{actual} = OC_A - OC_C$). Teflon filters were changed about once a week, even though it was shown (see below) that the amount of loading on the Teflon filter did not significantly affect the results. Additional artifact measurements were made by sampling with configurations B and C concurrently.

**Analysis Protocol Comparison.** Three different temperature profiles, a modified-NIOSH protocol, a modified-IMPROVE protocol, and a FAST-ramp protocol, were compared. Temperature profiles and purge gases in each analysis stage of these methods are presented in Table 1. The modified-NIOSH method is adapted from the NIOSH temperature profile (*14*, *42*) and was used by Schauer et al. (*26*). The modified-IMPROVE method is adapted from the IMPROVE protocol (*16*, *26*). The methods differ only in the temperatures used in the He atmosphere of the first analysis part. The FAST-ramp method requires an analysis step of only 4 min and takes advantage of the optical measurements to enable this shorter analysis time. In this method, the sample is heated quickly to 850 °C in a 10% oxygen in helium atmosphere in only one step and TC is quantified from the total NDIR response. EC is measured optically, on the basis of initial and final laser transmittance, and is then used to determine OC via subtraction from TC. The faster analysis reduces the time when sampling is interrupted and also increases the sensitivity dramatically, since all carbon evolves in one narrow peak. Thus, it may allow for shorter, subhourly sampling times.

For all the temperature profile comparisons, denuders were used on both monitors (configuration B) since, as

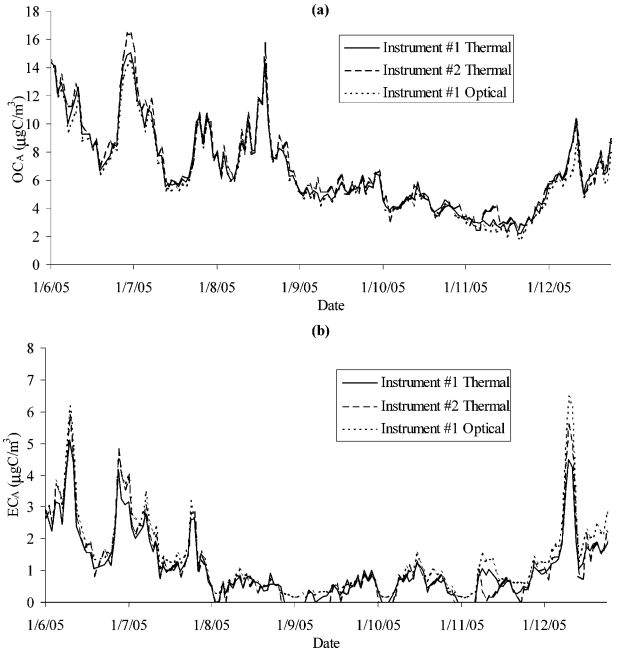


**FIGURE 2. Test of instrumental precision results for (a) OC measurements and (b) EC measurements.**

described later, this was shown to provide nearly artifact free sampling. Except for these temperature protocol comparisons, all other samples in this study were analyzed using the modified-NIOSH protocol. In both the modified-NIOSH and modified-IMPROVE methods, the four temperature steps in the He atmosphere allow for division of OC into different NDIR response peaks representing different volatility fractions of OC (*43*). These four OC peaks are designated and recorded as peak 1 to peak 4 ($OC^1$ to $OC^4$). For the purposes of this study, $OC^2$, $OC^3$, and $OC^4$ were summed ($OC^{2-4}$) and considered a less volatile OC fraction compared to $OC^1$, a more volatile OC fraction.

**Comparison of Quasi-Ultrafine Particles with Accumulation Mode Particles.** Two collocated instruments provided the opportunity for simultaneous semicontinuous EC/OC measurements of different PM size fractions. The $PM_{0.25}$ stage of a Sioutas impactor (SKC Inc., Eighty Four, PA) (*44*, *45*) was operated downstream of the PM2.5 cyclone of one of the instruments to remove particles greater than 250 nm in aerodynamic diameter (configuration E, Figure 1e). Considering that the upper size cuts that have been traditionally used to define the ultrafine mode (100−180 nm) are somewhat lower than the cutpoint of the Sioutas impactor (*46*−*48*), particles less than 250 nm are designated quasi-ultrafine (UF) for the purposes of this paper ($OC_E = OC_{uf}$, $EC_E = EC_{uf}$). The measurements with the UF inlet configuration were subtracted from the concurrent $PM_{2.5}$ measurements (configuration B) to obtain accumulation mode (0.25−2.5 $\mu$m) carbon values ($OC_{acc} = OC_B - OC_E$, $EC_{acc} = EC_B - EC_E$).

## Results and Discussion

**Precision Evaluation.** The time series plots of OC and EC measured concurrently by two collocated Sunset Laboratory semicontinuous OC/EC field analyzers using the bare configuration (A) are shown in Figure 2. Thermal OC measurements between the two instruments were very highly correlated with a correlation coefficient, $R^2$, of 0.98, a slope of 1.01 ± 0.02, and *y*-intercept of 0.12 ± 0.16 $\mu$g C/m$^3$. The $R^2$, slope, and *y*-intercept of measured EC with the two instruments were 0.97, 0.82 ± 0.02, and 0.2 ± 0.04 $\mu$g C/m$^3$, respectively. The results show excellent interinstrument precision for OC, but a systematic bias in EC is reflected in the slope of 0.82. The reason for this discrepancy might be a result of a systematic difference in the split point determination between OC and EC, and as the EC values are a much lower fraction of TC, EC is affected to a greater degree than OC. The split point between OC and EC of the instrument with overall higher EC measurements (instrument #2) occurred on average 17 s before the split point of the other instrument (instrument #1). Also, there were periods with relatively low levels of EC during the comparison, which were close to the detection limit of the instrument (0.2 $\mu$g C/m$^3$ according to manufacturer), which may cause additional uncertainty in the readings. At some of these low EC levels, when the EC level was near the detection limit, the instrument was unable to properly detect the split between EC and OC. In these cases, the split point between OC and EC for at least one of the monitors occurred at the end of the analyzing period, which resulted in artificially lower EC measurements (practically zero EC levels). Therefore, the EC measurements for which the split point occurred at the end of analyzing period were considered outliers and excluded from the analysis. This occurrence was infrequent, resulting in exclusion of less than 5% of data.

Total carbon measured by the two instruments correlated well, with $R^2$ and slope of 0.99 and 0.94 ± 0.02, respectively. Slightly lower TC measurements occurred on the same instrument with the overall higher split point. The lower TC measurements in this unit combined with the effect of the higher split point resulted in lower EC measurements. For OC, these two effects approximately cancel each other out, since lower EC now corresponds to higher OC.

The ability of the analyzers to measure EC (and by subtraction OC) optically was also assessed by comparing the thermal data of each instrument to its own optical data. The $R^2$ and slope of thermal versus optical OC correlation were 0.98 and 1.04 ± 0.02 for one unit and 0.99 and 0.98 ± 0.02 for the other unit. Comparisons of thermal and optical EC yielded an $R^2$ and slope of 0.97 and 0.77 ± 0.04 for one unit and 0.97 and 0.98 ± 0.05 for the second instrument. These results indicate very strong correlation between optical and thermal measurements. However, in one of the instruments, the optical EC values seem to be higher compared to thermal EC, and because optical OC is determined by subtraction, the optical OC values are lower than thermal OC on the same instrument. As optical EC measured by the two units correlated well with each other with a slope close to 1 ($R^2$ =1.00, slope = 1.07 ± 0.03), the observed difference in optical and thermal EC measurements in one of the units is caused by the lower thermal EC measurements of this unit mentioned above. The EC concentrations measured thermally with each unit were also compared to BC measurements done with the Aethalometer. The $R^2$ and slope of correlation between BC and EC were 0.96 and 1.39 ± 0.06, respectively, for one unit and 0.95 and 1.17 ± 0.05 for the other. This indicates a high correlation between EC and BC measurements, which was also shown in several previous studies (*28*, *29*, *36*−*38*), but systematically lower EC measurements than BC.

**Denuder Breakthrough.** Denuder breakthrough was assessed using configuration D (Figure 1d). The average OC, EC, $OC^1$, and $OC^{2-4}$ measured with this configuration are presented in Table 2. The fact that no EC was measured implies the perfect removal of particles by the Teflon filter, so the measured value of OC originated solely from organic gases penetrating through the denuder and adsorbing to the quartz filter (*30*, *31*, *39*). The average of the OC measurements was 0.82 ± 0.31 $\mu$g C/m$^3$ and the $R^2$ between the bare OC measurements and $OC_D$ was 0.01, with a slope of 0.01 ± 0.07, which together indicate a fairly constant degree of breakthrough adsorption, unrelated to ambient particulate OC

**TABLE 2. Average Denuder Breakthrough Values, Which Were Subtracted from All Denuded Samples (all values in $\mu$g C/m$^3$)**

| parameter | average | standard deviation |
|---|---|---|
| OC | 0.82 | 0.31 |
| EC | 0.00 | 0.00 |
| $OC^1$ | 0.43 | 0.10 |
| $OC^{2-4}$ | 0.37 | 0.17 |

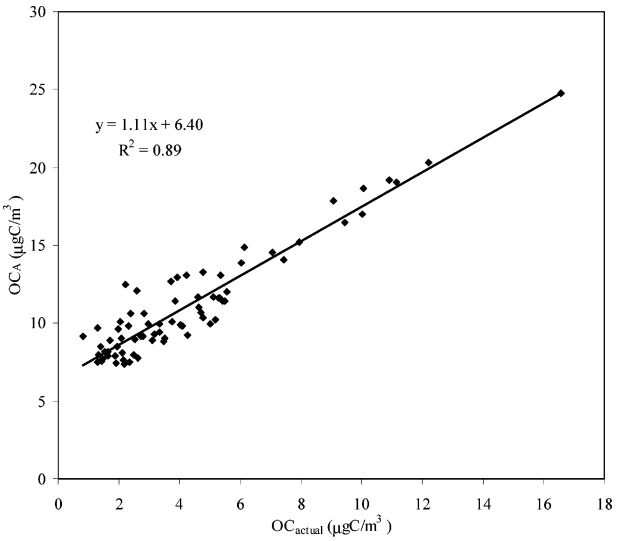


**FIGURE 3. The comparison between the bare OC ($OC_A$) and the particulate OC obtained from the Teflon filter method ($OC_{actual}$) concurrently.**

levels. The average denuder breakthrough of 0.82 $\mu$g C/m$^3$ was therefore subtracted from all the OC measurements obtained by using the denuder. The average denuder breakthroughs for $OC^1$ and $OC^{2-4}$ were 0.43 $\pm$ 0.10 and 0.37 $\pm$ 0.17 $\mu$g C/m$^3$, respectively. As was done for total OC, the average $OC^1$ breakthrough was subtracted from all the $OC^1$ measurements and the average $OC^{2-4}$ breakthrough was subtracted from $OC^{2-4}$ measurements of samples collected with a denuder upstream. The sum of $OC^1$ and $OC^{2-4}$ breakthrough is smaller than the average of total OC breakthrough because of the small amount of pyrolyzed OC included in total OC but not in OC peaks 1−4.

**Sampling Artifacts.** Using the filter method to determine the OC sampling artifact as described above, the positive artifact ($OC_C = OC_{artifact,filter}$) ranged from 5.1 to 8.9 $\mu$g C/m$^3$, while the concurrent $OC_A$ from the bare configuration ranged from 7.2 to 24.7 $\mu$g C/m$^3$. The average $EC_C$ was less than 0.01 $\mu$g C/m$^3$, which demonstrated the high efficiency of particle removal by the Teflon filter. The results of actual particulate OC ($OC_{actual} = OC_A - OC_C$) obtained by the Teflon filter method and concurrent bare OC measurements ($OC_A$) are shown in Figure 3. A fairly high correlation with $R^2$ of 0.89 was found between $OC_{actual}$ and $OC_A$ with a high nonzero intercept. Since the bare $OC_A$ consists of both positive artifacts and particulate OC, the high correlation and slope near unity show that the variation of $OC_A$ is driven by variations in particulate OC. An approximate estimate of the level of positive artifact is indicated by the intercept at 6.4 $\mu$g C/m$^3$.

Operating one instrument with a denuder configuration (B) concurrently with the other instrument in the bare configuration (A) provides another measure of the magnitude of sampling artifacts. In this case, the artifact will include potentially enhanced negative artifacts caused by the denuder (*31*, *40*, *41*). If an initial assumption is made that the negative artifact is negligible, then $OC_{actual} = OC_B$, and the positive artifact is then $OC_{artifact,denuder} = OC_A - OC_B$. As shown, the

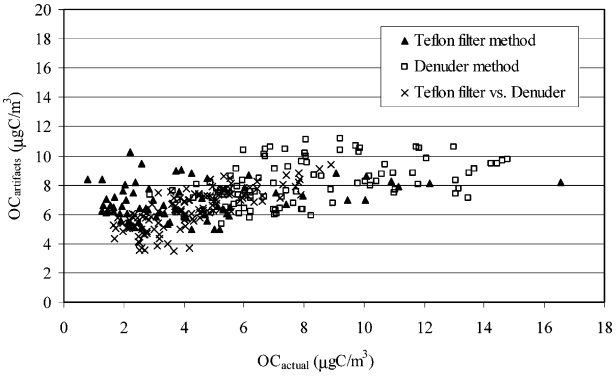


**FIGURE 4. Comparison between $OC_{artifact}$ and $OC_{actual}$ determined by the Teflon filter method (configuration A vs C), denuder method (configuration A vs B), and concurrent usage of Teflon filter and denuder (configuration C vs B).**

filter method arrives at the same parameters ($OC_{actual} = OC_A - OC_C$, $OC_{artifact,filter} = OC_C$), and the results from both artifact determination methods are plotted in Figure 4. The amount of positive artifact does not correlate well with the actual particulate OC ($R^2 = 0.26$), and only a slight increase in positive artifact was observed for increasing the actual OC level (slope = 0.22). The average of the positive artifacts measured with both methods was 7.59 $\pm$ 1.52 $\mu$g C/m$^3$, with average $OC_{artifact,denuder}$ and $OC_{artifact,filter}$ of 8.14 $\pm$ 1.49 and 6.86 $\pm$ 1.21 $\mu$g C/m$^3$, respectively. The average positive artifact determined using the denuder method is about 1.3 $\mu$g C/m$^3$ higher than the artifact using the filter method, but within the standard deviation of the measurements. This difference could be due to the negative artifact associated with the denuder, which would lead to an overestimation of the positive artifact by that method. However, it should also be noted that the measurements using the two methods were conducted over two different sampling periods, with higher particulate OC levels during the denuder method sampling. The average bare OC during the denuder method measurements was 16.24 $\mu$g C/m$^3$ compared to 11.14 $\mu$g C/m$^3$ with the filter method. Higher OC levels during the denuder method sampling period could lead to slightly higher artifacts due to possibly higher organic vapor concentrations on more polluted days and/or possible matrix adsorption effects (*43*).

The observed differences between the two methods does provide a rough upper estimate of the negative artifact of approximately 1 $\mu$g C/m$^3$, less than 20% of the positive artifact on average. Other studies have demonstrated similar results for negative artifacts on 24-h samples, e.g. less than 10% of particulate OC by Subramanian et al. (*31*). However, higher negative artifacts (up to 80% of particulate OC) were also measured in other studies, which indicates a wide range of negative artifacts based on site and sampling conditions (*31*, *49*−*52*). Also shown in Figure 4 are results from measurements with one of the instruments operating with a Teflon filter (configuration C) concurrently with the other instrument operating with a denuder (configuration B). The measured $OC_C$ ($OC_{artifact,filter}$) is plotted as function of the measured $OC_B$ ($OC_{actual}$). An average positive artifact of 6.33 $\pm$ 1.34 $\mu$g C/m$^3$ was observed, which was consistent with our results using the filter and denuder methods separately, as can be seen in Figure 4.

The positive artifact was relatively high compared to actual particulate OC, comprising approximately 50% of $OC_A$ on average. This large value for positive artifacts is attributable to the short 45-min sampling time. Organic gases will adsorb on the filter until the filter is fully saturated (*31*). The longer sampling continues after saturation occurs, the lower the positive artifact will be relative to actual particulate OC. Thus, a 24-h sample would have a lower artifact relative to actual

particulate OC than a 45-min sample, assuming filter saturation is reached within 24 h. The high percentage of artifact observed here indicates that the bare configuration of these instruments cannot directly measure actual particulate OC reliably.

If the sampling time is long enough for the quartz filter to saturate with adsorbed organic vapors, then the artifact mass will remain constant (*31*). For a short sampling time of 45 min, it is assumed that gas-phase organic concentrations do not vary sufficiently to cause additional adsorption or volatilization of organic material due to the changing vapor pressures of these gases. As stated above, the average 7.59 $\mu$g C/m$^3$ positive artifact was measured for a 45-min sampling period. This corresponds to an adsorption artifact on the filter of 0.68 $\mu$g C/cm$^2$ (two back-to-back 16-mm filters, 8 L/min, and a 45-min sample). In a previous study in the Los Angeles basin, the average measured positive artifact was 1.3 $\mu$g/m$^3$ for 24-h sampling on 37-mm quartz filters with 30 L/min flow rate (*33*). This corresponds to 5.22 $\mu$g C/cm$^2$, which is about 7.7 times the artifact value determined in this study. In another study in the same basin, an average positive artifact of 2.17 $\mu$g C/m$^3$ was obtained (*53*), this time based on a flow rate of 20 L/min, 24-h sampling, and using 47-mm filters. This value corresponds to 3.6 $\mu$g C/cm$^2$ of positive OC artifact, which is about 5.3 times the artifacts measured here. Comparison of our results with both of these studies indicates that the saturation condition was probably not achieved in 45 min of sampling.

To verify whether saturation was achieved, the samples were collected for 165 min of sampling period and analyzed in 15 min (total cycle of 3 h) using configurations B and C concurrently. The average positive artifacts of 54 samples collected in May 2005 was 4.51 $\pm$ 0.94 $\mu$g C/m$^3$, corresponding to a 1.62 $\mu$g C/cm$^2$ of positive OC artifact, which is 2.4 times higher than the artifacts measured for a sampling period of 45 min. This result further indicates that the filters were not saturated within 45 min. While the sampling period was increased about 3.7 times, the artifacts were enhanced only 2.4 times, suggesting that the adsorption rate of gas-phase organics slows as sampling continues. In a previous study in Pittsburgh (*31*), an average positive artifact of 0.53 and 0.71 $\mu$g C/m$^3$ was found respectively for 24 h and 4−6 h of sampling with 47-mm quartz filters and a 16.7 L/min flow rate, corresponding to filter artifacts of 0.75 and 0.21 $\mu$g C/cm$^2$, respectively. In that study, filter saturation was not achieved after 6 h of sampling. As in our case, the artifact concentration on the filter increased with increasing sampling time, but the adsorption rate slows down as it approaches saturation conditions. Differences in the magnitude of the positive artifacts and adsorption rates at different locations indicate that the amount of OC artifact can vary significantly with sampling conditions. This is probably due to differences in concentrations of gas-phase organics at different sites and seasons.

An overcorrection of positive artifacts using the filter method was predicted in previous studies (*31*, *54*) due to organic particulate matter collected on the Teflon filter volatilizing and then adsorbing to the quartz filter downstream. This effect was examined by operating two instruments side-by-side using configuration C, initially both having new Teflon filters. After about 60 h, sufficient time for Teflon filters to be heavily loaded with particulate matter, the Teflon filter on one of the instruments was changed while the other one remained unchanged, then 20 samples were collected on each instrument. The average difference between the OC measured by the two instruments before the filter change was low (0.55 $\pm$ 0.52 $\mu$g C/m$^3$) and nearly identical to the difference after the filter change (0.58 $\pm$ 0.57 $\mu$g C/m$^3$). The similarity indicates that this effect may not be important for the current study, and that an overestimation of positive artifacts by using a loaded Teflon filter upstream has not occurred.

The relationship between particulate OC obtained by the Teflon method and bare $OC_A$ (shown in Figure 3) may provide a correction to estimate actual particulate OC in cases when the denuder is not deployed. The validity of this correction is demonstrated in Figure 5, where particulate OC, calculated from $OC_A$ and the linear relationship in Figure 3, is compared to particulate OC measured concurrently with a denuder ($OC_B$, ignoring the negligible negative artifact). The time series (Figure 5a) confirms the good agreement. Figure 5b compares the calculated and measured OC in a scatter plot, showing a high correlation with a slope of 0.98 $\pm$ 0.08. This good agreement shows that it may be possible to obtain good particulate OC results in a bare configuration, using a previously derived correction. The derived linear relationship between the particulate OC and the bare OC may be specific to particular sampling site, instrument configuration, and/or sampling duration. The excellent agreement in Figure 5b also shows that the negative artifact caused by using a denuder is minor and does not significantly effect the particulate OC measurements. Therefore, the denuder configuration provides the best measure of actual particulate OC without significant associated artifacts.

**Temperature Profiles.** Table 3 shows the statistical comparison of measurements made with the modified-IMPROVE and the FAST-ramp methods run concurrently with the modified-NIOSH method. The OC analyzed by the modified-IMPROVE protocol showed a good agreement with the OC measured by using the modified-NIOSH protocol with an $R^2$ of 0.93 and slope of 1.04, consistent with a previous study by Chow et al. (*23*). The main difference between methods is the maximum temperature reached in the first analysis stage: 550 °C for the modified-IMPROVE and 850 °C in the modified-NIOSH method. This shows that a temperature of 550 °C is enough to evolve almost all of the OC. The EC temperature steps in both methods are the same, so any observed difference is the result of a difference between the split points affected by potentially more pyrolysis of OC at the higher temperatures of the modified-NIOSH method. Considering the $R^2$ of 0.92 and slope of 1.05 for EC measurements, and similar results for OC and TC, the two methods compare very well under the conditions of our experiments.

The OC measured using the FAST-ramp temperature program (TC − optical EC) also correlated well with concurrent thermal OC measurements by the modified-NIOSH method with a correlation coefficient of 0.92. The slope of 0.90 (0.87, 0.94) indicates slightly lower OC measurements compared to the modified-NIOSH method. The EC measurements in contrast were higher than those of the modified-NIOSH method with a slope of 1.38 but a high correlation coefficient of 0.98. TC measurements were also fairly consistent, with an $R^2$ of 0.98 and slope of 1.08. The FAST-ramp relies on the optical EC measurement to determine both EC and OC levels. The optical EC measurement is based on a manufacturer calibration, derived from relating differences in laser transmission to thermally measured EC levels over many samples using the modified-NIOSH profile. Comparing the optical EC measurements via the FAST method with optical EC measurements via NIOSH method, an $R^2$ of 1.00 and slope of 0.99 (0.99, 1.00) were obtained. This excellent correlation is a result of using the same procedure for determining optical EC in both instruments in either of the methods. The systematic bias between optical and thermal EC measurements of about 30% in one of the units (used for the modified-NIOSH method in this comparison) observed earlier during the instrumental precision tests can explain most of the difference between EC by the FAST-ramp and thermal EC by modified-NIOSH. The OC

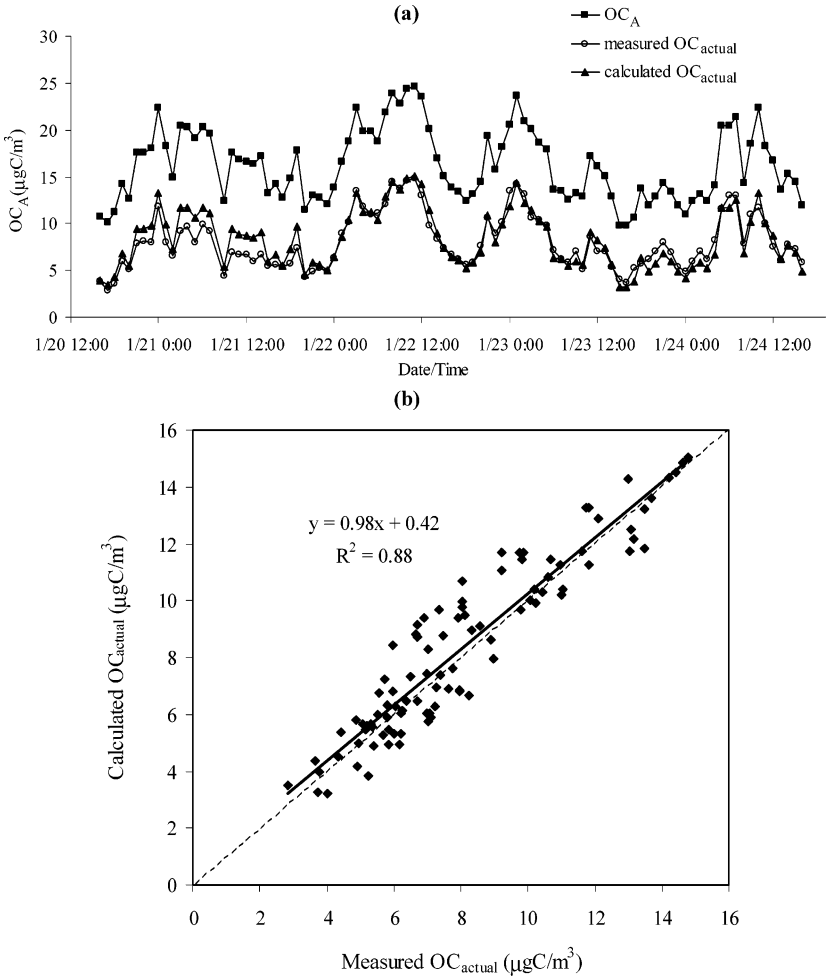


**FIGURE 5. Calculated $OC_{actual}$ from bare configuration measurements (applying the relationship found with the Teflon filter method) compared to $OC_{actual}$ measured with a denuder: (a) time series data including the uncorrected bare OC ($OC_A$) and (b) correlation plot.**

**TABLE 3. Comparison between Measured Carbonaceous Components of $PM_{2.5}$ by Different Methods (units in $\mu$g C/m$^3$)**

| protocol | no. of samples | compared parameter | $R^2$ | slope (95% intervals) | intercept (95% intervals) |
|---|---|---|---|---|---|
| modified-IMPROVE vs modified-NIOSH | 114 | OC | 0.93 | 1.04 (0.99, 1.10) | 0.09 (−0.11, 0.30) |
| | | EC | 0.92 | 1.05 (1.11, 1.00) | 0.24 (0.17, 0.31) |
| | | TC | 0.95 | 1.08 (1.04, 1.13) | 0.13 (−0.10, 0.35) |
| FAST-ramp vs modified-NIOSH | 236 | OC | 0.92 | 0.90 (0.87, 0.94) | 0.05 (−0.2, 0.09) |
| | | EC | 0.98 | 1.38 (1.35, 1.4) | −0.14 (−0.17, −0.11) |
| | | optical OC | 0.91 | 1.13 (1.08, 1.18) | −0.59 (−0.42, −0.77) |
| | | optical EC | 1.00 | 0.99 (0.99, 1.00) | −0.08 (−0.09, −0.07) |
| | | TC | 0.98 | 1.08 (1.05, 1.10) | −0.59 (−0.71, −0.47) |

measurements by the FAST method are also highly correlated with optical OC via the NIOSH method with an $R^2$ and slope of 0.91 and 1.13 respectively, which are close to the correlation between TC measurements of these two methods ($R^2 = 0.98$ and slope =1.08). This indicates that the difference between these two optical OC values mainly originates from the difference between TC measurements, since optical EC values were shown to be similar. The high correlation between EC measured with the NIOSH and FAST protocols suggests that a new calibration would bring the results into better agreement. Given these encouraging results, the shorter analysis time in the FAST-ramp method will potentially allow for nearly continuous sampling or shorter sampling periods.

**Size-Fractionated Measurements.** The instrument with a quasi-ultrafine inlet and denuder configuration (configuration E) was run concurrently with the other instrument in a $PM_{2.5}$ denuder configuration (configuration B), and 387 hourly samples were collected in March and May of 2005. The hourly OC measured in the quasi-ultrafine (UF) mode ranged from 0.03 to 5.80 $\mu$g C/m$^3$ with average of 1.59 $\mu$g C/m$^3$. Similar results were found in the accumulation mode, with OC ranging from 0.07 to 8.49 $\mu$g C/m$^3$ with an average of 1.37 $\mu$g C/m$^3$. The hourly EC in the quasi-ultrafine mode varied from 0.32 to 5.20 $\mu$g C/m$^3$ with an average of 1.16 $\mu$g C/m$^3$. EC in the accumulation mode was significantly less, varying from 0.0 to 2.78 $\mu$g C/m$^3$ with an average of 0.49 $\mu$g C/m$^3$. The average diurnal variations of particulate OC and EC in the both size ranges are presented in Figure 6. The diurnal variations of particulate EC as well as OC in these two size fractions generally track each other well. The significant morning peak indicates the effect of morning rush hour. The UF concentrations of OC reached the maximum about 1 h earlier than the accumulation mode concentrations. A possible explanation is that UF particles are freshly emitted particles, originating directly from nearby emissions of mobile sources and thus have diurnal patterns that follow traffic

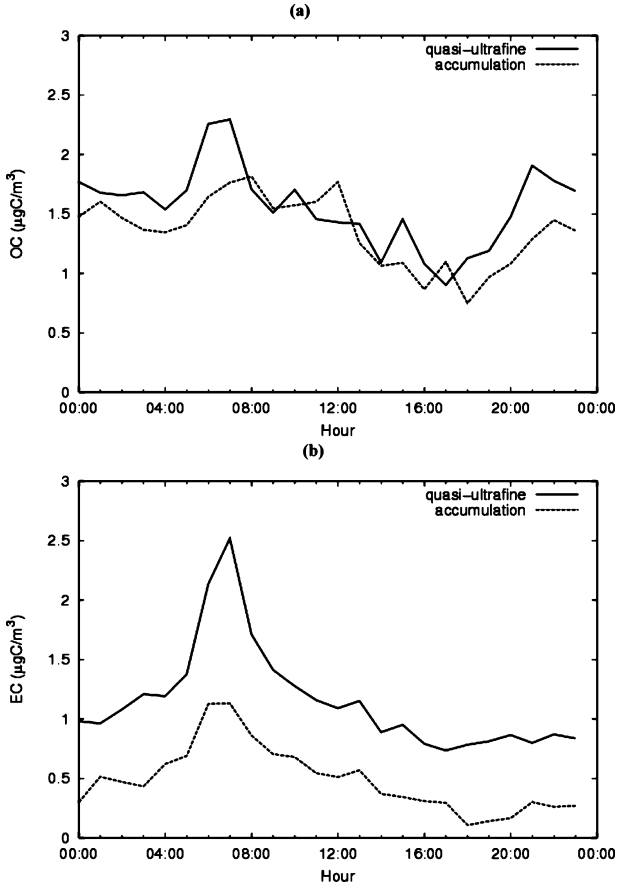


**FIGURE 6. The diurnal pattern of carbonaceous component of particles in quasi-ultrafineand accumulation mode: (a) OC and (b) EC.**

volume. By contrast, accumulation-mode PM, which may have been emitted earlier as smaller particles in locations upwind of our sampling site, may be reaching the site after aging in the atmosphere, a process that allows for condensation of organic vapors onto preexisting particles and thus an increase in particle size.

The $OC^1$ concentration (more volatile OC) in the UF mode varied between 0.01 and 3.26 $\mu$g C/m$^3$ with an average of 0.67 $\mu$g C/m$^3$, while $OC^1$ in the accumulation mode was higher, ranging from 0.07 to 4.78 $\mu$g C/m$^3$ with an average of 0.96 $\mu$g C/m$^3$. The $OC^{2-4}$ (less volatile OC) in the UF mode ranged from 0.02 to 2.54 $\mu$g C/m$^3$ with an average of 0.93 $\mu$g C/m$^3$, with lower values in the accumulation mode between 0.0 and 3.68 $\mu$g C/m$^3$ with the average of 0.41 $\mu$g C/m$^3$. The average ratios of $OC^1$ and $OC^{2-4}$ to total particulate OC in the UF and accumulation modes are presented in Figure 7. The average EC/OC ratios of particles in the UF and accumulation mode are also displayed in the same figure. The considerably higher EC to OC ratio in the UF mode is due to the different sources and formation process of the two particle size ranges. EC from mobile sources (in the form of soot) is emitted primarily in smaller particles (*55*, *56*). While OC is also emitted in smaller particles from mobile sources, a portion of accumulation-mode OC is formed by the condensation of organic gases that were either directly emitted from mobile sources or formed by photochemical secondary reactions (*56*). The higher $OC^1$/OC and lower $OC^{2-4}$/OC in the accumulation mode compared to the UF mode indicates higher OC volatility in the accumulation mode. This is consistent with OC condensation in this mode, since both photochemical products and condensable vapors from vehicles are often semivolatile species that will partition to pre-existing particle surface area (*56*).

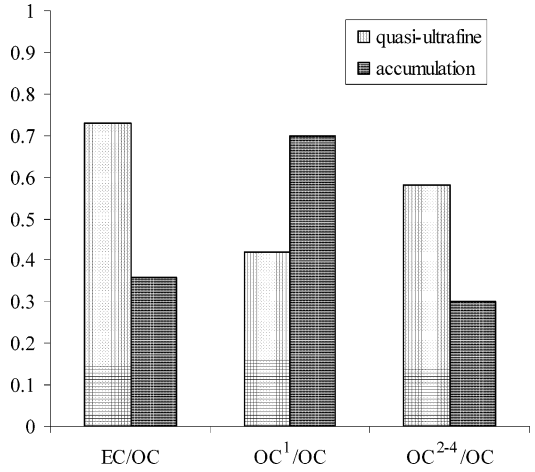


**FIGURE 7. The ratio of particulate EC, $OC^1$, and $OC^{2-4}$ to particulate OC in quasi-ultrafine and accumulation modes.**

## Acknowledgments

This research was supported by grant number ES06214 from the National Institute of Environmental Health Sciences (NIEHS), U.S. National Institutes of Health (NIH), and the California Air Resources Board through subcontract Nos. 53-4507-1420 and 53-4507-0841 to the University of Southern California. The contents are solely the responsibility of the authors and do not necessarily represent the official views of the NIEHS, NIH. The statements and conclusions described herein have not been subjected to review and comment by CARB and therefore do not necessarily reflect the views of the agency, and no official endorsement should be inferred. Mention of trade names or commercial products does not constitute an endorsement or recommendation for use.

## Literature Cited

(1) NRC. *Research Priorities for Airborne Particulate Matter: IV. Continuing Research Progress*; Committee on Research Priorities for Airborne Particulate Matter; National Research Council: Washington, DC, 2004.

(2) Batalha, J. R. F.; Saldiva, P. H. N.; Clarke, R. W.; Coull, B. A.; Stearns, R. C.; Lawrence, J.; Murthy, G. G. K.; Koutrakis, P.; Godleski, J. J. Concentrated ambient air particles induce vasoconstriction of small pulmonary arteries in rats. *Environ. Health Perspect.* **2002**, *110*, 1191−1197.

(3) Clarke, R. W.; Coull, B.; Reinisch, U.; Catalano, P.; Killingsworth, C. R.; Koutrakis, P.; Kavouras, I.; Murthy, G. G. K.; Lawrence, J.; Lovett, E.; Wolfson, J. M.; Verrier, R. L.; Godleski, J. J. Inhaled concentrated ambient particles are associated with hematologic and bronchoalveolar lavage changes in canines. *Environ. Health Perspect.* **2000**, *108*, 1179−1187.

(4) Saldiva, P. H. N.; Clarke, R. W.; Coull, B. A.; Stearns, R. C.; Lawrence, J.; Murthy, G. G. K.; Diaz, E.; Koutrakis, P.; Suh, H.; Tsuda, A.; Godleski, J. J. Lung inflammation induced by concentrated ambient air particles is related to particle composition. *Am. J. Resp. Crit. Care Med.* **2002**, *165*, 1610−1617.

(5) Wellenius, G. A.; Coull, B. A.; Godleski, J. J.; Koutrakis, P.; Okabe, K.; Savage, S. T.; Lawrence, J. E.; Murthy, G. G. K.; Verrier, R. L. Inhalation of concentrated ambient air particles exacerbates myocardial ischemia in conscious dogs. *Environ. Health Perspect.* **2003**, *111*, 402−408.

(6) Burnett, R. T.; Brook, J.; Dann, T.; Delocla, C.; Philips, O.; Cakmak, S.; Vincent, R.; Goldberg, M. S.; Krewski, D. Association between particulate- and gas-phase components of urban air pollution and daily mortality in eight Canadian cities. *Inhalation Toxicol.* **2000**, *12*, 15−39.

(7) Mar, T. F.; Norris, G. A.; Koenig, J. Q.; Larson, T. V. Associations between air pollution and mortality in Phoenix, 1995−1997. *Environ. Health Perspect.* **2000**, *108*, 347−353.

(8) Metzger, K. B.; Tolbert, P. E.; Klein, M.; Peel, J. L.; Flanders, W. D.; Todd, K.; Mulholland, J. A.; Ryan, P. B.; Frumkin, H. Ambient air pollution and cardiovascular emergency department visits. *Epidemiology* **2004**, *15*, 46−56.

(9) Dejmek, J.; Solansky, I.; Benes, I.; Lenicek, J.; Sram, R. J. The impact of polycyclic aromatic hydrocarbons and fine particles on pregnancy outcome. *Environ. Health Perspect.* **2000**, *108*, 1159−1164.
(10) Li, N.; Sioutas, C.; Cho, A.; Schmitz, D.; Misra, C.; Sempf, J.; Wang, M. Y.; Oberley, T.; Froines, J.; Nel, A. Ultrafine particulate pollutants induce oxidative stress and mitochondrial damage. *Environ. Health Perspect.* **2003**, *111*, 455−460.
(11) Oberdörster, G. Pulmonary effects of inhaled ultrafine particles. *Int. Arch. Occup. Environ. Health* **2001**, *74*, 1−8.
(12) Tesfaigzi, Y.; Singh, S. P.; Foster, J. E.; Kubatko, J.; Barr, E. B.; Fine, P. M.; McDonald, J. D.; Hahn, F. F.; Mauderly, J. L. Health effects of subchronic exposure to low levels of wood smoke in rats. *Toxicol. Sci.* **2002**, *65*, 115−125.
(13) Seagrave, J.; Knall, C.; McDonald, J. D.; Mauderly, J. L. Diesel particulate material-binds and concentrates a proinflammatory cytokine that causes neutrophil migration. *Inhalation Toxicol.* **2004**, *16*, 93−98.
(14) Birch, M. E.; Cary, R. A. Elemental carbon-based method for monitoring occupational exposures to particulate diesel exhaust. *Aerosol Sci. Technol.* **1996**, *25*, 221−241.
(15) Chow, J. C.; Watson, J. G. PM2.5 carbonate concentrations at regionally representative Interagency Monitoring of Protected Visual Environment sites. *J. Geophys. Res.*—Atmos. **2002**, *107*.
(16) Chow, J. C.; Watson, J. G.; Pritchett, L. C.; Pierson, W. R.; Frazier, C. A.; Purcell, R. G. The DRI Thermal Optical Reflectance Carbon Analysis System—Description, Evaluation and Applications in United-States Air-Quality Studies. *Atmos. Environ. Part a*—Gen. Top. **1993**, *27*, 1185−1201.
(17) Oberdörster, G.; Sharp, Z.; Atudorei, V.; Elder, A.; Gelein, R.; Lunts, A.; Kreyling, W.; Cox, C. Extrapulmonary translocation of ultrafine carbon particles following whole-body inhalation exposure of rats. *J. Toxicol. Environ. Health*—Part A **2002**, *65*, 1531−1543.
(18) Hildemann, L. M.; Klinedinst, D. B.; Klouda, G. A.; Currie, L. A.; Cass, G. R. Sources of Urban Contemporary Carbon Aerosol. *Environ. Sci. Technol.* **1994**, *28*, 1565−1576.
(19) Griffin, R. J.; Dabdub, D.; Kleeman, M. J.; Fraser, M. P.; Cass, G. R.; Seinfeld, J. H. Secondary organic aerosol—3. Urban/regional scale model of size- and composition-resolved aerosols. *J. Geophys. Res.*—Atmos. **2002**, *107*.
(20) Reisen, F.; Arey, J. Atmospheric reactions influence seasonal PAH and nitro-PAH concentrations in the Los Angeles basin. *Environ. Sci. Technol.* **2005**, *39*, 64−73.
(21) Schauer, J. J.; Rogge, W. F.; Hildemann, L. M.; Mazurek, M. A.; Cass, G. R. Source apportionment of airborne particulate matter using organic compounds as tracers. *Atmos. Environ.* **1996**, *30*, 3837−3855.
(22) Hughes, L. S.; Allen, J. O.; Kleeman, M. J.; Johnson, R. J.; Cass, G. R.; Gross, D. S.; Gard, E. E.; Galli, M. E.; Morrical, B. D.; Fergenson, D. P.; Dienes, T.; Noble, C. A.; Silva, P. J.; Prather, K. A. Size and composition distribution of atmospheric particles in southern California. *Environ. Sci. Technol.* **1999**, *33*, 3506−3515.
(23) Chow, J. C.; Watson, J. G.; Crow, D.; Lowenthal, D. H.; Merrifield, T. Comparison of IMPROVE and NIOSH carbon measurements. *Aerosol Sci. Technol.* **2001**, *34*, 23−34.
(24) Chow, J. C.; Watson, J. G.; Chen, L. W. A.; Arnott, W. P.; Moosmuller, H. Equivalence of elemental carbon by thermal/optical reflectance and transmittance with different temperature protocols. *Environ. Sci. Technol.* **2004**, *38*, 4414−4422.
(25) Birch, M. E. Analysis of carbonaceous aerosols: Interlaboratory comparison. *Analyst* **1998**, *123*, 851−857.
(26) Schauer, J. J.; Mader, B. T.; Deminter, J. T.; Heidemann, G.; Bae, M. S.; Seinfeld, J. H.; Flagan, R. C.; Cary, R. A.; Smith, D.; Huebert, B. J.; Bertram, T.; Howell, S.; Kline, J. T.; Quinn, P.; Bates, T.; Turpin, B.; Lim, H. J.; Yu, J. Z.; Yang, H.; Keywood, M. D. ACE-Asia intercomparison of a thermal-optical method for the determination of particle-phase organic and elemental carbon. *Environ. Sci. Technol.* **2003**, *37*, 993−1001.
(27) Schmid, H.; Laskus, L.; Abraham, H. J.; Baltensperger, U.; Lavanchy, V.; Bizjak, M.; Burba, P.; Cachier, H.; Crow, D.; Chow, J.; Gnauk, T.; Even, A.; ten Brink, H. M.; Giesen, K. P.; Hitzenberger, R.; Hueglin, E.; Maenhaut, W.; Pio, C.; Carvalho, A.; Putaud, J. P.; Toom-Sauntry, D.; Puxbaum, H. Results of the "carbon conference" international aerosol carbon round robin test stage I. *Atmos. Environ.* **2001**, *35*, 2111−2121.
(28) Hansen, A. D. A.; Rosen, H.; Novakov, T. The Aethalometer—An Instrument for the Real-Time Measurement of Optical-Absorption by Aerosol-Particles. *Sci. Total Environ.* **1984**, *36*, 191−196.
(29) Lim, H. J.; Turpin, B. J.; Edgerton, E.; Hering, S. V.; Allen, G.; Maring, H.; Solomon, P. Semicontinuous aerosol carbon measurements: Comparison of Atlanta Supersite measurements. *J. Geophys. Res.*—Atmos. **2003**, *108*.
(30) Bae, M. S.; Schauer, J. J.; DeMinter, J. T.; Turner, J. R.; Smith, D.; Cary, R. A. Validation of a semi-continuous instrument for elemental carbon and organic carbon using a thermal-optical method. *Atmos. Environ.* **2004**, *38*, 2885−2893.
(31) Subramanian, R.; Khlystov, A. Y.; Cabada, J. C.; Robinson, A. L. Positive and negative artifacts in particulate organic carbon measurements with denuded and undenuded sampler configurations. *Aerosol Sci. Technol.* **2004**, *38*, 27−48.
(32) McDow, S. R.; Huntzicker, J. J. Vapor Adsorption Artifact in the Sampling of Organic Aerosol − Face Velocity Effects. *Atmos. Environ. Part a-Gen. Top.* **1990**, *24*, 2563−2571.
(33) Sardar, S. B.; Fine, P. M.; Sioutas, C. Seasonal and spatial variability of the size-resolved chemical composition of particulate matter (PM10) in the Los Angeles Basin. *J. Geophys. Res.*—Atmos. **2005**, *110*.
(34) Jeong, C. H.; Lee, D. W.; Kim, E.; Hopke, P. K. Measurement of real-time PM2.5 mass, sulfate, and carbonaceous aerosols at the multiple monitoring sites. *Atmos. Environ.* **2004**, *38*, 5247−5256.
(35) Manual Semi-Continuous OCEC Carbon Aerosol Analyzer; Sunset Laboratory Inc., 2004.
(36) Turpin, B. J.; Cary, R. A.; Huntzicker, J. J. An Insitu, Time-Resolved Analyzer for Aerosol Organic and Elemental Carbon. *Aerosol Sci. Technol.* **1990**, *12*, 161−171.
(37) Lavanchy, V. M. H.; Gäggeler, H. W.; Nyeki, S.; Baltensperger, U. Elemental carbon (EC) and black carbon (BC) measurements with a thermal method and an aethalometer at the high-alpine research station Jungfraujoch. *Atmos. Environ.* **1999**, *33*, 2759−2769.
(38) Ballach, J.; Hitzenberger, R.; Schultz, E.; Jaeschke, W. Development of an improved optical transmission technique for black carbon (BC) analysis. *Atmos. Environ.* **2001**, *35*, 2089−2100.
(39) Turpin, B. J.; Saxena, P.; Andrews, E. Measuring and simulating particulate organics in the atmosphere: Problems and prospects. *Atmos. Environ.* **2000**, *34*, 2983−3013.
(40) Eatough, D. J. A., N.; Cottam, M.; Gammon, T.; Hansen, L. D.; Lewis, E. A.; Farber, R. J. In *Loss of semi-volatile organic compounds from particles during sampling on filters;* Mathai, C. V., Ed.; Air and Waste Management Association: Pittsburgh, PA, 1990; pp 146−156.
(41) Turpin, B. J.; Huntzicker, J. J.; Hering, S. V. Investigation of organic aerosol sampling artifacts in the Los Angeles basin. *Atmos. Environ.* **1994**, *28*, 3061−3071.
(42) NIOSH In *Book Elemental carbon* (*diesel particulate*)*: Method 5040*; 4th ed. (1st supplement); NIOSH: Cincinnati, 1996.
(43) Kirchstetter, T. W.; Corrigan, C. E.; Novakov, T. Laboratory and field investigation of the adsorption of gaseous organic compounds onto quartz filters. *Atmos. Environ.* **2001**, *35*, 1663−1671.
(44) Misra, C.; Singh, M.; Shen, S.; Sioutas, C.; Hall, P. A. Development and evaluation of a personal cascade impactor sampler (PCIS). *J. Aerosol Sci.* **2002**, *33*, 1027−1047.
(45) Singh, M.; Misra, C.; Sioutas, C. Field evaluation of a personal cascade impactor sampler (PCIS). *Atmos. Environ.* **2003**, *37*, 4781−4793.
(46) Chakrabarti, B.; Singh, M.; Sioutas, C. Development of a near-continuous monitor for measurement of the sub-150 nm PM mass concentration. *Aerosol Sci. Technol.* **2004**, *38*, 239−252.
(47) Fine, P. M.; Chakrabarti, B.; Krudysz, M.; Schauer, J. J.; Sioutas, C. Diurnal variations of individual organic compound constituents of ultrafine and accumulation mode particulate matter in the Los Angeles basin. *Environ. Sci. Technol.* **2004**, *38*, 1296−1304.
(48) Kim, S.; Shen, S.; Sioutas, C.; Zhu, Y. F.; Hinds, W. C. Size distribution and diurnal and seasonal trends of ultrafine particles in source and receptor sites of the Los Angeles basin. *J. Air Waste Manage. Assoc.* **2002**, *52*, 297−307.
(49) Anderson, R. R.; Martello, D. V.; Rohar, P. C.; Strazisar, B. R.; Tamilia, J. P.; Waldner, K.; White, C. M.; Modey, W. K.; Mangelson, N. F.; Eatough, D. J. Sources and composition of PM2.5 at the National Energy Technology Laboratory in Pittsburgh during July and August 2000. *Energy Fuels* **2002**, *16*, 261−269.
(50) Ding, Y. M.; Pang, Y. B.; Eatough, D. J. High-volume diffusion denuder sampler for the routine monitoring of fine particulate matter: I. Design and optimization of the PC−BOSS. *Aerosol Sci. Technol.* **2002**, *36*, 369−382.
(51) Eatough, D. J.; Wadsworth, A.; Eatough, D. A.; Crawford, J. W.; Hansen, L. D.; Lewis, E. A. A Multiple-System, Multichannel Diffusion Denuder Sampler for the Determination of Fine-

Particulate Organic Material in the Atmosphere. *Atmos. Environ. Part a*—Gen. Top. **1993**, *27*, 1213−1219.
(52) Modey, W. K.; Pang, Y.; Eatough, N. L.; Eatough, D. J. Fine particulate (PM2.5) composition in Atlanta, USA: Assessment of the particle concentrator-Brigham Young University organic sampling system, PC−BOSS, during the EPA supersite study. *Atmos. Environ.* **2001**, *35*, 6493−6502.
(53) Kim, B. M.; Cassmassi, J.; Hogo, H.; Zeldin, M. D. Positive organic carbon artifacts on filter medium during PM2.5 sampling in the South Coast Air Basin. *Aerosol Sci. Technol.* **2001**, *34*, 35−41.
(54) Chow, J. C.; Watson, J. G.; Lu, Z. Q.; Lowenthal, D. H.; Frazier, C. A.; Solomon, P. A.; Thuillier, R. H.; Magliano, K. Descriptive analysis of PM(2.5) and PM(10) at regionally representative locations during SJVAQS/AUSPEX. *Atmos. Environ.* **1996**, *30*, 2079−2112.
(55) Kittelson, D. B. Engines and Nanoparticles: A Review. *J. Aerosol Sci.* **1998**, *29*, 575−588.
(56) Kleemann, M. J. Source contributions to the size and composition distribution of atmospheric particles: Southern California in September 1996. *Environ. Sci. Technol.* **1999**, *33*, 4331−4341.

*Received for review June 1, 2005. Revised manuscript received November 8, 2005. Accepted November 20, 2005.*

ES0510313